Published in final edited form as:
Dev Cell. 2008 January ; 14(1): 108–119. doi:10.1016/j.devcel.2007.11.004.

The BMP signaling gradient patterns dorsoventral tissues in a temporally progressive manner along the anteroposterior axis

Jennifer A. Tucker, **Keith A. Mintzer**, and **Mary C. Mullins***
University of Pennsylvania School of Medicine, Department of Cell and Developmental Biology, 1211 BRBII/III, Philadelphia, PA 19104-6058, USA

Summary

Patterning of the vertebrate anteroposterior (AP) axis proceeds temporally from anterior to posterior. How dorsoventral (DV) axial patterning relates to AP temporal patterning is unknown. We examined the temporal activity of BMP signaling in patterning ventrolateral cell fates along the AP axis, using transgenes that rapidly turn 'off' or 'on' BMP signaling. We show that BMP signaling patterns rostral DV cell fates at the onset of gastrulation, while progressively more caudal DV cell fates are patterned at progressively later intervals during gastrulation. Increased BMP signal duration is not required to pattern more caudal DV cell fates, rather distinct temporal intervals of signaling are required. This progressive action is regulated downstream of, or in parallel to BMP signal transduction at the level of Smad1/5 phosphorylation. We propose that a temporal cue regulates a cell's competence to respond to BMP signaling, allowing the acquisition of a cell's DV and AP identity simultaneously.

INTRODUCTION

A gradient of BMP signaling specifies cell fates along the DV axis, with the highest levels specifying the ventral-most tissues, while increasing BMP inhibition leads to more lateral tissues and an absence of BMP signaling to dorsal tissues in the ectoderm and mesoderm of both frogs and fish (Dosch et al., 1997; Knecht and Harland, 1997; LaBonne and Bronner-Fraser, 1998; Marchant et al., 1998; Neave et al., 1997; Wilson et al., 1997). Targeted mutations of BMP signaling components in the mouse also indicate a role for BMP signaling in DV patterning in mammals; however, embryonic lethality of these mutations prior to gastrulation has precluded more in-depth studies (reviewed in Zhao, 2003). In zebrafish, mutations in BMP signaling components have permitted genetic analysis of their roles in DV patterning in vertebrates (reviewed in Little and Mullins, 2006). Null mutations of the zebrafish BMP ligands, *bmp2b (swirl)* and *bmp7 (snailhouse),* the type I BMP receptor *alk8* (*lost-a-fin*), and the intracellular signal transducer, *smad5 (somitabun),* all display strongly dorsalized phenotypes, whereby dorsally-derived neural tissue and somitic mesoderm is circumferentially expanded at the expense of ventrally-derived epidermis, blood, tail, and laterally-derived cranial neural crest and pronephros (Bauer et al., 2001; Hild et al., 1999; Kishimoto et al., 1997; Kramer et al., 2002; Mintzer et al., 2001; Mullins et al., 1996; Nguyen et al., 1998b; Schmid et al., 2000). Recent morpholino knockdowns reveal a similar role for the BMP ligands,

*Correspondence: mullins@mail.med.upenn.edu

together with ADMP, in DV patterning in Xenopus (Reversade and De Robertis, 2005; Reversade et al., 2005).

Models of DV patterning by the BMP morphogen gradient are static in the nature of their function, with gradient function depicted at a single time point patterning all DV cells. However, signaling by morphogen gradients involves questions of timing. The formation of a morphogen gradient cannot occur instantaneously, and hence cells cannot take their reading of morphogen level too early, or too late, after a putative gradient collapses or is distorted by morphogenesis as development proceeds. Thus, it is crucial to determine the influence of timing on cell fate specification during morphogen gradient signaling.

The temporal action of the BMP signaling gradient in DV patterning has been examined in several contexts. BMP activity has been visualized in *Xenopus* by spatial distribution of phosphorylated Smad1/5, with high levels ventrally and low levels dorsally throughout gastrulation (Faure et al., 2000; Schohl and Fagotto, 2002), delineating a potentially long window of time available for cells to respond to BMP signaling. Studies in *Xenopus* and zebrafish using inducible BMP components show that BMP inhibition initiated during mid-blastula stages disrupts DV axial patterning (Marom et al., 2005; Pyati et al., 2005; Wawersik et al., 2005). In fish, BMP signaling sets aside tail progenitors during early gastrulation (Agathon et al., 2003), then patterns these progenitors into ventral tail tissues during early somitogenesis (Connors et al., 2006; Pyati et al., 2005). Thus, current models of the temporal requirements for BMP signaling imply only a coarse temporal program wherein a BMP signaling gradient patterns the DV axis of the entire embryo, aside from the tail, at a single interval prior to or during gastrulation.

In contrast, patterning of cell fates along the orthogonal anteroposterior (AP) axis occurs in a clear temporal fashion from anterior to posterior (reviewed in Stern et al., 2006). No prior studies have addressed the relationship between the temporal patterning of cells along the AP and DV axes. To determine the temporal requirements for BMP signaling, and if cells integrate BMP signals with temporal AP patterning, we generated heat-shock inducible transgenes that can rapidly activate or inhibit BMP signaling. In a careful series of BMP inhibition studies, we discovered that ventrolateral ectodermal and mesodermal cell fates are not patterned simultaneously over the entire AP extent of the embryo. Rather, BMP signaling acts in a temporally progressive manner, required earliest in anterior ventrolateral cells and subsequently in progressively more posterior ventrolateral cells. We propose a model in which cells along the AP axis in the head and trunk respond to the BMP signaling gradient during progressively later, distinct critical intervals, a mechanism allowing cells to adopt both an AP and DV identity simultaneously, thus coordinating patterning of these two axes.

RESULTS

Formation of the BMP activity gradient

To visualize formation of the BMP activity gradient, we examined the spatial distribution of phosphorylated Smad1/5 (P-Smad5), the transcription factor activated via phosphorylation by the type I BMP receptor. During mid-blastula stages (prior to 4 hpf), P-Smad5 is equally distributed at low levels throughout the blastoderm (data not shown). At 4 hpf, a clearing begins to form on the dorsal side, and punctate nuclear staining is apparent throughout the remainder of the blastoderm (Fig. 1A). This dorsal clearing expands ventrally (Fig. 1B, C) forming a very shallow gradient. By the onset of gastrulation (5.5 hpf), P-Smad5 is restricted to the ventral side of the embryo, with intensity increasing in the extreme ventral region (Fig. 1D), forming a steep gradient that persists throughout gastrulation (Fig 1E, F, G, H). After the onset of gastrulation, P-Smad5 becomes more restricted in ventral-vegetal regions, whereas it extends slightly more dorsally in animal regions (Fig. 1F, G, H), similar to *bmp* expression at these

stages (Dick et al., 2000;Kishimoto et al., 1997;Schmid et al., 2000). During early to mid-gastrulation stages (6 to 7 hpf), nearly all ventral ectodermal cells at all positions along the animal-vegetal axis, as well as involuted mesendodermal cells are positive for P-Smad5 (Fig S1A-L). We examined a series of animal-view confocal sections spanning from the animal pole to the margin and found that lateral cells at all animal-vegetal positions were positive for P-Smad5 at both early and mid-gastrulation (6 to 7.25 hpf, data not shown). At the end of gastrulation, P-Smad5 decreases in ventral-animal regions (Fig 1I). The early formation of a P-Smad5 gradient suggests that BMP signaling may specify cell fates as early as late blastula stages. Alternatively, the P-Smad5 gradient may not be functional until the steep, more ventrally restricted gradient has formed at the onset of gastrulation. Furthermore, although the presence of P-Smad5 indicates that a cell has received and activated BMP signaling, it does not demonstrate when such signaling is required for patterning.

BMP signaling through Alk8 is first required at the onset of gastrulation

To determine when BMP signaling first functions to pattern ventrolateral tissues, we determined the temporal requirement for the type I Bmp receptor Alk8 (Lost-a-fin) in DV patterning. Maternal-zygotic *lost-a-fin* (MZ-*laf*) mutants display a strongly dorsalized class 5 (C5) phenotype, the strongest in our dorsalization series (Mullins et al. 1996), in which dorsal neural tissue expands dramatically into ventral regions (Fig. 2A, F insets, Mintzer et al., 2001). We generated transgenic lines of the *alk8* cDNA under the control of the *heat-shock70-inducible* promoter (Halloran et al., 2000), Tg(*hsp70:alk8*), in an *alk8 (laf)* heterozygous background. When Tg(*hsp70:alk8*); *laf*/+ males were crossed to *laf* homozygous females (laf^{m100}/laf^{tm110b}), 50% of the progeny displayed a C5 phenotype in the absence of heat-shock, indicating no expression of the paternally provided transgene when not induced (Fig. 2A). The remaining 50% are wild-type due to zygotic rescue by the wild-type *alk8* (*laf*) paternal chromosome.

We then examined the ability of Tg(*hsp70:alk8*) to rescue MZ-*laf* mutants at various time points during development. We confirmed rescue of MZ-*laf* mutants by genotyping (data not shown). Heat-shock induction (HS) of the transgene during blastula stages (4 hpf) rescued the C5 dorsalized phenotype in 100% of MZ-*laf* embryos (Fig 2D, n=37) and had no effect on maternal-*laf* (M-*laf*) embryos (Fig 2B, C); however, only 14% of MZ-*laf* embryos were fully rescued to wild-type. The remaining embryos lacked ventral tail tissues at 24 hpf (Fig 2E), indicative of a weak class 1 or 2 dorsalization and partial rescue by Tg(*hsp70:alk8)*. HS during early gastrulation (6 hpf) rescued the C5 dorsalized phenotype in 85% of MZ-*laf* embryos (n=26), with 58% of embryos rescued to wild-type. In all rescued embryos, neurectoderm and paraxial mesoderm domains returned to wild-type (Fig 2D, inset, data not shown). MZ-*laf* mutant embryos displayed little or no P-Smad5 during early gastrulation in the absence of transgene induction (Fig 2G, H, Mintzer et al., 2001). In contrast, a robust gradient was observed 30 minutes (min) following the onset of Tg(*hsp70:alk8*) induction and in early gastrulation in MZ-*laf* mutant embryos (Fig 2I, K), similar to wild-type embryos (Fig 2J), demonstrating the ability to rapidly re-initiate signaling at the onset of gastrulation. HS at mid-gastrulation (6.5 or 7 hpf) failed to rescue MZ-*laf* embryos to any extent (n=27, data not shown, and n=22, Fig 2F). These results indicate that cells begin to integrate BMP activity at or just following the onset of gastrulation, coinciding with the appearance of the steep PSmad5 gradient. Moreover, the gradient formed prior to gastrulation provides little or no DV patterning information.

Alk8 patterns tail tissues during early somitogenesis

HS at early gastrulation only rescued a fraction of MZ-*laf* embryos to a wild-type phenotype. This 30-min HS may not supply high enough levels of Alk8 or alternatively, as BMP signaling patterns tail tissues after gastrulation (Connors et al., 2006; Pyati et al., 2005), *alk8* mRNA or

protein may not be sufficiently stable to pattern the tail, if only transcribed at early gastrulation. To test if Alk8 functions at a later stage to pattern tail tissues, we heat-shocked MZ-*laf* mutant embryos for 30-min at a blastula stage (4 hpf) and at the end of gastrulation (10 hpf), which fully rescued all MZ-*laf* embryos, including tail tissues (n=14). We also investigated rescue by Tg(*hsp70-alk8*) of zygotic(Z)-*laf* mutants, which display a class 2 (C2) dorsalized phenotype restricted to the tail (Fig S2A, Mullins et al., 1996). HS during gastrulation (5-10 hpf) and as late as the 1-somite stage (10.5 hpf) rescued Z-*laf* mutants to wild-type (confirmed by genotyping; Fig 2L, S2B). Between the 2- and 9-somite stage (11-13 hpf), rescue decreased significantly (Fig 2L, S2C, D). Thus, there are at least two periods when BMP activity patterns DV tissues: first during early gastrulation to pattern ventrolateral cranial and trunk tissues, and later during early somitogenesis to pattern the tail.

A rapid and robust inducible BMP inhibition system

Our MZ-*laf* rescue experiments determined the earliest requirement for BMP signaling in patterning ventrolateral tissues, but did not allow us to determine if posterior ventrolateral head and trunk tissues exhibit a later requirement for BMP signaling than anterior head ventrolateral cells. We reasoned that inhibiting BMP signaling at different time points would enable us to distinguish between three possible models, by more clearly establishing the timing of BMP signaling in patterning ventrolateral cell fates at different cranial and rostral trunk AP positions. In referring to head/cranial or trunk tissues here, we refer to these prospective tissues during late blastula and gastrula stages. In a first model, BMP signaling acts at a single time interval to pattern all head and trunk ventrolateral tissues. In this case, inhibition of BMP signaling prior to or during that single interval would result in complete dorsalization of both head and trunk tissues. Inhibiting BMP signaling after this interval would result in proper ventrolateral patterning along the entire head and trunk. In a second model, BMP signaling acts progressively over time, patterning anterior ventrolateral tissues first, and subsequently patterning more posterior ventrolateral domains at progressively later intervals. In this case, we expect that inhibiting BMP signaling prior to the earliest required interval will result in complete dorsalization at all AP positions, whereas later inhibition will allow proper ventrolateral patterning in the anterior-most positions, while posterior ventrolateral cells would remain dorsalized. A third model would include a combination of these two models, in which, for example, all head ventrolateral tissues are patterned during one time interval, followed by all trunk ventrolateral tissues patterned during a second interval.

To selectively inhibit BMP signaling, we generated transgenic fish carrying cDNA encoding the BMP antagonist *chordin* under the control of the *hsp70* promoter, Tg(*hsp70:chd*). Two Tg (*hsp70:chd*) lines were established, and we obtained similar results with both. Males carrying Tg(*hsp70:chd*) were crossed to *snh*(*bmp7*)$^{sb1aub/sb1aub}$ females, which enhanced the ability of Tg(*hsp70:chd*) to inhibit BMP signaling. Transgenic and non-transgenic *snh*^{sb1aub}/+ embryos show no dosage sensitivity to the partial loss of *bmp7*, displaying a completely wild-type phenotype in the absence of HS.

We tested the kinetics of our inhibitory system by first examining *chordin* mRNA induction. We found ubiquitous elevated *chd* expression within 30 min of the start of HS (Fig S3A, B). We examined P-Smad5 distribution and levels by whole mount immunohistochemistry and Western blot. The P-Smad5 gradient formed by 60 min post-HS in non-transgenic controls (Fig S3C, D) was absent in transgenic embryos (Fig S3E, n=6). For 60-min heat-shocks beginning at 4, 5, or 6 hpf, P-Smad5 levels were greatly reduced 40 min after the *start* of heat-shock (in this case, only a 40-min HS), and were absent by 60 min (Fig 3B), compared to wild-type where P-Smad5 levels steadily increased (Fig 3A). Thus Tg(*hsp70:chd*) can rapidly and completely inhibit BMP signaling.

Temporal BMP inhibition series phenocopies BMP mutants

Induction of Tg(*hsp70:chd*) for 60 min at various time points reproduces the range of dorsalized phenotypes observed in BMP mutants (Mullins et al., 1996). HS beginning in mid and late blastula stages, 4, 4.5, or 5 hpf, resulted in 100% or 95% of embryos displaying the characteristic elongated C5 dorsalized phenotype (Fig 3D, I) with all somites extending around the embryo circumference compared to non-transgenic embryos, which were unaffected by HS (Fig 3C). HS at the onset of, or early in gastrulation (5.5 or 6 hpf) resulted in slightly weaker C4 dorsalizations, in which the tail is absent and trunk tissues twist above the yolk (Fig. 3E, F, I). HS at 6 or 7 hpf resulted in C3 dorsalized embryos with a normal head and anterior trunk, but a dorsalized posterior trunk and tail (Fig 3G, I). These results are consistent with our MZ-*laf* rescue results, and together demonstrate that BMP signaling patterns DV tissues of the head and anterior trunk during early gastrulation. HS from mid-gastrulation (8 hpf) through the end of gastrulation (10 hpf) caused a C2 dorsalization restricted to the tail (Fig 3I). HS after gastrulation (11 hpf) up to the 6-somite stage (12 hpf) caused weaker C1 dorsalizations to the tail, whereas those after this stage had no effect on DV patterning (Fig 3H, I).

Thus, when BMP signaling is inhibited at progressively later stages, the strength of dorsalization becomes less severe. Posterior positions can be dorsalized by later HS, while anterior positions are not, consistent with the second and third models above, wherein the head and trunk are patterned during distinct temporal intervals.

Decreasing gastrula dorsalization in temporal BMP inhibition series

The progression to weaker dorsalized phenotypes observed in live Tg(*hsp70:chd*) embryos heat-shocked between 5.5 and 10 hpf suggests that embryos heat-shocked at earlier stages may also differ in DV patterning, despite their identical morphological appearance. To determine if this is the case, we analyzed gene expression during gastrulation. We examined the dorsally expressed gene *otx2* in the prospective fore- and mid-brain neurectoderm (Fig 4A, Li et al., 1994), *foxb1.2*, expressed in neural tissue posterior to the forebrain (Fig 4B,Odenthal and Nusslein-Volhard, 1998), and the ventral non-neural ectodermal markers, *AP-2* and *dlx3* (Fig 4C, D).

In embryos heat-shocked at 4 hpf (mid-blastula), *otx2* and *foxb1.2* expression domains extended fully to the ventral side (Fig 4E, F). Conversely, *AP-2* and *dlx3* expression was completely absent (Fig 4G, H), similar to C5 dorsalized *bmp2b* mutant embryos (Nguyen et al., 1998b). Embryos heat-shocked at 5 hpf (late blastula) were morphologically similar at 10 hpf to those heat-shocked at 4 hpf; however, during early gastrulation the extent of *otx2* expansion was reduced (Fig 4I), while *foxb1.2* expansion was similar to 4 hpf heat-shocked embryos (Fig 4J), consistent with weaker dorsalization in the anterior. Expression of *AP-2* and *dlx3* was absent (Fig 4K, L). Embryos heat-shocked at 5.5 hpf displayed normal *otx2* expression, whereas *foxb1.2* was expanded ventrolaterally, but not fully into ventral regions (Fig 4M, N). *AP-2* expression was absent (Fig 4O), whereas *dlx3* was expressed in a small ventral domain towards the animal pole (Fig 4P), indicative of ventral character in anterior regions. Embryos heat-shocked at 6 hpf had normal expression domains of *otx2* and *foxb1.2* (Fig 4Q, R), and both *AP-2* and *dlx3* were expressed, although in a more restricted ventral domain than in control embryos (Fig 4C, D, S, T). These results are consistent with later BMP inhibition leading to decreased dorsalization during gastrulation.

BMP inhibition series shows progressive temporal patterning along the AP axis

The Ectoderm—The changes in gastrula gene expression observed for heat-shocks between 4 and 6 hpf suggest that DV patterning may proceed progressively along the AP axis in prospective head regions, as postulated in model 2. To investigate if cranial ventrolateral tissues are patterned progressively, we examined the expression of ectodermal genes that require three

different levels of BMP signaling at different AP positions. *pax2.1* and *krox20* are expressed in the neurectoderm at the position of the midbrain-hindbrain boundary (MHB) and rhombomeres 3 and 5 (R3 and R5), respectively (Fig 5A, D), and require an absence of BMP signaling to be expressed. *foxd3* is expressed in cranial neural crest (CNC) prior to the 6-somite stage, which requires an intermediate level of BMP signaling (Fig 5B, D) (Nguyen et al., 1998a; Tribulo et al., 2003). *p63* is expressed at all AP positions in the epidermis (Fig 5C, D), which requires a high level of BMP signaling for its specification (Bakkers et al., 2002; Lee and Kimelman, 2002; Wilson et al., 1997).

HS beginning at 4 or 4.5 hpf caused complete expansion of neural markers and loss of CNC and epidermis at the AP positions of MHB, R3, and R5 (Fig 5E-H, data not shown), indicating complete dorsalization at all AP positions. HS at 5 hpf (late blastula) caused only partial expansion of neural tissue at the MHB position, but complete expansion at R3 and R5 positions (Fig 5I, L). Consistent with reduced anterior expansion of *otx2* during early gastrulation prior to convergent-extension movements (Fig 4I), the ventral-most anterior cells of 5 hpf heat-shocked embryos are specified as CNC, while epidermis is absent (Fig 5J, K, L). Since CNC is present only in the most anterior region of the embryo and the MHB is only partially expanded (Fig 5J, L), this indicates that the anterior MHB position is only weakly dorsalized, whereas the more posterior R3 and R5 positions are completely dorsalized.

HS beginning at 5.5 hpf (onset of gastrulation) resulted in partial expansion of neural tissue at the MHB and R3 positions, but complete expansion at the R5 position (Fig 5M, P). Accordingly, CNC was present in an expanded domain at the positions of MHB and R3, but absent at the R5 position (Fig 5N, P). Examination of *crestin* expression in the trunk neural crest (NC) posterior to rhombomere 4 (Nguyen et al., 2000; Rubinstein et al., 2000) confirmed loss of posteriorly-positioned NC (Fig. S4A-E). Epidermis was present in a few cells in the most anterior position (Fig 5O, P). These results show a weaker dorsalization at the MHB and R3 than at R5 and more posterior regions (Fig 5P). HS at 6 hpf (shield stage) resulted in nearly wild-type domains of neurectoderm, CNC, and epidermis at the positions of MHB and R3 (Fig 5Q-T), moderate expansion of CNC at and posterior to the position of R5 (Fig 5R, T), and loss of epidermis posterior to R5 (Fig 5S, T). Finally, HS at 6.5 hpf resulted in wild-type domains of neurectoderm, CNC, and epidermis at all AP positions except for the most posterior region that will give rise to posterior trunk and tail (Fig 5U-X). Thus, all ventrolateral cells in the prospective head and anterior trunk have responded to the BMP signaling gradient by 7 to 7.5 hpf, the time we expect the BMP signaling gradient to be inhibited following a heat-shock starting at 6.5 hpf (Fig. 3). Furthermore, these studies show that in cranial regions, the BMP signaling gradient functions progressively over time to pattern DV tissues along the AP axis, with more anteriorly positioned ventrolateral cells being patterned prior to more posteriorly positioned ones.

The mesoderm—We also investigated the temporal requirements of BMP signaling in patterning ventrolateral mesoderm at different trunk AP positions. We examined *WT1* (Fig 6A) and *pax2.1* (Fig 6B) expression in the pronephros. *WT1* is expressed lateral to somites 1-4, whereas *pax2.1* is expressed lateral to somite 3 and extends posteriorly (Serluca and Fishman, 2001). We also examined the ventrally-derived blood precursors via *gata1* expression (Fig 6C), which begins at the boundary between somites 5 and 6 and extends posteriorly (data not shown). *myoD* expression in the dorsally-derived somites does not require BMP signaling and was used to determine the extent of dorsalization in the mesoderm at different AP positions (data not shown). HS at 4 hpf caused complete loss of *WT1*, *pax2.1*, and *gata1* expression, and the reciprocal circumferential expansion of all somites (data not shown). HS at 5 hpf resulted in *WT1* expression in a ventrally-shifted and expanded domain (Fig 6D), and loss of the more posterior *pax2.1* and *gata1* domains (Fig 6E, F). Somite 1 was expanded, but did not encircle the embryo, whereas more posterior somites did. HS at 5.5 hpf resulted in a more restricted

WT1 expression domain anteriorly (Fig 6G), but expansion posteriorly, and continued loss of *gata1* expression (Fig 6I). Pronephric *pax2.1* expression was present in 5.5 hpf HS embryos in two of four experiments (Fig 6H), suggesting that 5.5 hpf is very close to the critical interval when BMP signaling specifies these most anterior *pax2.1*-pronephric cells. In these embryos, *pax2.1* was expressed in only the most anterior cells of the domain and was ventrally shifted, whereas *myoD* expression in somites 4 and posteriorly encircled the embryo. Finally, HS at 6 hpf resulted in nearly wild-type *WT1* expression (Fig 6J), ventrally-shifted and anteriorly restricted expression of *pax2.1* and *gata1* (Fig 6K, L), and normal or mildly expanded *myoD* expression in somites 1-4. These results indicate that similar to the ectoderm, DV patterning of mesodermal tissues occurs progressively over time along the AP axis.

Distinct temporal intervals, not increased BMP signal duration pattern more posterior DV cell fates

Our BMP inhibition results do not address if posterior ventrolateral tissues require a longer duration of BMP signaling to be specified or if they require signaling during a later temporal interval than more anterior ventrolateral tissues. In our MZ-*laf* rescue experiments, posterior positions were not rescued without rescue of anterior positions. However, this lack of rescue is difficult to interpret because *bmp* ligand gene expression is under a positive autoregulatory feedback mechanism, such that in the absence of BMP signaling, as in the MZ-*laf* mutant, *bmp* expression is shut off during early gastrulation (Kramer et al., 2002; Nguyen at al. 1998; Schmid et al. 2000; Reversade and DeRobertis, 2005). Thus the failure to rescue MZ-*laf* mutants with *alk8* heat-shock induction at 6.5 hpf could be due to lack of BMP ligand availability. To overcome this difficulty we injected *bmp2b* mRNA into MZ-*laf* mutant embryos, which alone did not rescue the MZ-*laf* C5 dorsalized phenotype (Fig 6M). We then heat-shocked *bmp2b*-injected MZ-*laf* embryos carrying Tg(*hsp70:alk8*) at 6.75 hpf, and found that P-Smad5 was restored immediately after the 30 min heat-shock (Fig 6O), indicating that BMP signaling can be reinitiated at this stage, if ligand is present. Examination of *krox20* expression shows that R3 is completely expanded circumferentially, whereas the more posterior R5 is not and is partially rescued (Fig 6N, n=7). Since P-Smad5 is absent in MZ-*laf* embryos at 6.5 hpf (Fig 2H), these results indicate that the more posterior R5 position does not require BMP signaling prior to this point. These results indicate that the later temporal requirement for BMP signaling in more posterior ventrolateral positions is not due to a longer duration of BMP signal required for their specification, but rather that more posterior cells require BMP signaling during a later temporal interval.

DISCUSSION

Here we show that BMP signaling specifies ventrolateral cell fates in prospective cranial and rostral trunk regions not during one window of time, but instead, progressively more posterior ventrolateral cell fates are specified during progressively later temporal intervals during gastrulation. This unexpected coordination in patterning of the DV and AP axes may allow cells to adopt both an AP and DV identity simultaneously.

Recent results in *Xenopus* suggest that the axis traditionally defined as DV may represent the AP axis, with more dorsally located cells contributing to anterior positions (Reviewed in Lane and Sheets, 2006). However, zebrafish fate maps reveal a true dorsoventral axis perpendicular to the AP axis during gastrulation (Kimmel et al. 1990, Kozlowski et al. 1997, Woo and Fraser, 1995). In our Tg(*hsp70:chd*) embryos, as well as in BMP mutant embryos (Barth et al. 1999, Nguyen et al. 2000), we observe an expansion of dorsal neural tissue ventrally along the DV axis at the expense of ventrolaterally-derived gastrula cell fates. However, no change is observed in AP patterning, e.g. each rhombomere along the AP axis is specified correctly. BMP signaling does not function in the establishment of anterior cell identity per se, rather it patterns

ventrolateral cell fates in anterior regions, specifying NC, epidermis, blood, and pronephros, and restricting neural tissue to dorsal domains.

A model for Progressive Response to BMP signaling based on AP position

Taking into account the kinetics of our BMP inhibition system, our results are summarized in a model in Figure 7. The embryo is broadly divided into sectors reflecting DV and AP position (Fig 7A). The DV position of a single cell in each sector, and thus the level of BMP activity the cell experiences during gastrulation dictates the cell's fate, as either neurectoderm (no BMP activity, cells 3, 6, 9), CNC (intermediate BMP activity, cells 2, 5, 8), or epidermis (high BMP activity, cells 1, 4, 7) (Fig 7A). We then plotted the levels of BMP activity that each prospective cell type will experience over time from mid-blastula (4 hpf), when low level signaling is first detected, through mid-gastrulation (7 hpf) (Fig 7B). By the onset of gastrulation at 5.5 hpf, a BMP gradient is established such that ventrolateral cells exposed to an intermediate and high BMP level become CNC and epidermis, respectively, while dorsal cells, exposed to little or no signal, become neural tissue. Cells positioned along the AP axis at the MHB, R3, and R5 positions, each interpret the BMP signaling gradient during different critical intervals, as indicated by vertical rectangles at the MHB, R3, and R5 positions in Figure 7B. In wild-type, the shape of the gradient remains fairly constant from early to mid-gastrulation, thus generating the proper DV fate of each cell at the three AP positions over time.

In Tg(*hsp70:chd*) embryos heat-shocked at mid to late blastula (4 or 4.5 hpf) (Fig 7C), BMP signaling is inhibited by 5 or 5.5 hpf, prior to the complete formation of the P-Smad5 gradient, and all cells become neurectoderm. As BMP signaling is inhibited at a series of time points during gastrulation, complete dorsalization becomes restricted to progressively more posterior regions, indicating that ventrolateral cell fates in posterior regions have not yet been established by the BMP signaling gradient at the time of its inhibition, while anterior ventrolateral cell fates have. We observed moderate to mild dorsalization in anterior regions at progressively later BMP inhibition time points, indicating that the critical interval for these cells to respond to BMP signaling has passed, and they have become refractory to a decrease in BMP activity (Fig 7D-F). The moderate to mild dorsalization of anterior positions observed with BMP inhibition during early gastrulation (HS at 5 to 6 hpf), is likely due to the function of the reduced BMP signaling levels (P-Smad5) observed during the first 40 min of HS (Fig 3). Therefore, at the critical interval for a particular AP position, the slope of the BMP gradient has likely shifted, changing the BMP activity level each cell experiences to a level normally found in a more lateral position, leading to a cell fate change to one of a more lateral position, as illustrated in Fig 7D-F.

For example, a HS at 5.5 hpf (Fig 7E), which begins to affect BMP signaling levels 20 to 40 min later, partially inhibits BMP signaling during the critical interval for MHB position patterning, greatly inhibits signaling during the later critical interval for R3 position patterning, and completely blocks all BMP signaling during the critical interval for R5 position ventrolateral patterning. Hence, at the MHB position, the epidermis is greatly reduced, the CNC expanded ventrolaterally, and the neurectoderm expanded laterally. This same 5.5 hpf HS leads to greater inhibition of BMP signaling during the later critical interval for R3 (40 min post HS), leading to partially expanded neural tissue, ventrally shifted CNC, and loss of epidermis. Finally, during the critical interval for R5, 60-80 min following HS, BMP signaling is fully inhibited, leading to complete expansion of neural tissue and loss of CNC and epidermis at all AP positions at and posterior to R5 (Fig 7E). With a HS after the critical intervals of MHB and hindbrain, these AP positions are all wild-type along their DV axis, and dorsalization is restricted to the trunk and tail (Fig 7G).

Our results indicate that more posterior cells of a particular ventrolateral cell type do not require a longer duration of signal, but instead require signaling during a later temporal interval for

their specification. Since the P-Smad5 gradient does not change significantly between early and mid-gastrulation and ventrolateral cells converge dorsally very little or not at all during this period (Myers, et al., 2002; Sepich et al., 2000; von der Hardt et al., 2007), our results suggest that all ventrolateral cells along the AP axis during early to mid-gastrulation receive and transduce the BMP signal, phosphorylating Smad5, but they are not specified by it during the same temporal interval. Rather, progressively more posterior ventrolateral cell fates require BMP signaling at progressively later temporal intervals. For example, our results are consistent with a model wherein anterior and posterior CNC specification requires an intermediate level of BMP signaling for the same length of time, but for posterior CNC this time period begins later in gastrulation. This contrasts temporal aspects of other morphogen patterning systems. For example, during AP patterning of the hindbrain by retinoic acid (RA), posterior expression of *hoxd4a* requires not only a higher level of RA, but also a longer time of exposure to RA (Maves and Kimmel, 2005). A similar scenario occurs in mouse digit patterning by Sonic Hedgehog (Shh), where the middle digits integrate the time and level of exposure to Shh (Harfe et al., 2004).

Our results are generally consistent with other results examining the temporal action of BMP signaling in DV patterning. Strongly dorsalized phenotypes are observed for mid-blastula induction of a dominant-negative BMP receptor transgene in zebrafish (Pyati et al., 2005). Moderate to strong dorsalizations are generated with hormone inducible inhibitory Smads, Smad6 or a novel Smad7 form, during mid-blastula stages in Xenopus (Marom et al., 2005; Wawersik et al., 2005). Our inducible BMP inhibition system, *Tg(hsp70:chd)*, may be the most effective and rapid of currently reported ones, based on its ability to cause a loss of P-Smad5 within less than one hour of heat-shock onset, and its ability to induce the strongest dorsalization molecularly and morphologically at multiple timepoints, thus having the ability to inhibit all BMP signaling throughout the period of DV patterning.

Progressive BMP patterning of ectoderm is concurrent with the mesoderm

Interestingly, the sequential patterning that we observe in the mesoderm beginning at the first somite occurs in a similar timeframe as DV patterning of the MHB ectoderm. It has been suggested that DV patterning of the mesoderm drives DV patterning of the overlying ectoderm (Bonstein et al., 1998; Marchant et al., 1998). However, it is unlikely to explain our results, as zebrafish embryos that lack mesoderm still retain substantial DV patterning (Gritsman et al., 1999; Ragland and Raible, 2004; Tribulo et al., 2003). Similar to the coincident DV patterning of somite 1 and the MHB positions, DV patterning of R3 AP position ectoderm correlates with somite 3 position mesodermal patterning, and R5 position ectodermal patterning with somite 5-6 position patterning. Fate map analysis has revealed that at 6 hpf, precursors for anterior somites are close to the MHB and hindbrain precursors (Kimmel et al., 1990; Woo and Fraser, 1995). Thus, head ectoderm and trunk mesoderm may be patterned into DV cell fates by BMP signaling at the same time based on their similar relative cell positions during the time frame we investigated.

Dynamic integration of AP and DV patterning

In *Drosophila*, the BMP homologues Decapentaplegic and Screw act as morphogens to pattern the DV axis (reviewed by O'Connor et al., 2006). *Drosophila* embryos undergoes long germband embryogenesis, whereby all segments along the AP axis are generated simultaneously (Sander, 1976). However, in vertebrates, formation of the AP axis occurs over time in an anterior to posterior fashion, necessitating a temporal coordination of pattern formation along the AP and DV axes that is not required in *Drosophila*.

A model developed by Nieuwkoop proposes that in AP neural patterning in amphibians an activating factor neuralizes the ectoderm, followed by a transforming factor that posteriorizes

it (Nieuwkoop, 1950). Our results indicate that BMP signaling functions at the onset of gastrulation to restrict neuralization to dorsal regions at, and anterior to the position of the MHB, but not in more posterior regions although BMP signal transduction is evident by P-Smad5 in these regions. Thus, neural tissue can still be induced in ventral regions posterior to the MHB position by BMP inhibition after the onset of gastrulation, whereas more anterior tissues are now refractory to changes in BMP signaling. Our results indicate that the restriction of neuralization to dorsal regions, and perhaps neuralization itself, occurs in a temporally progressive manner along the AP axis.

To our knowledge, our results represent the first evidence of a temporal link between patterning DV cell fates in head and rostral trunk and their independent AP axial patterning in vertebrates. We postulate that posteriorization or AP patterning of neural tissue, which occurs with a temporal progression from anterior to posterior (Erter et al., 2001; Gamse and Sive, 2000; Gamse and Sive, 2001; Kudoh et al., 2002), is coordinated with the progressive DV patterning that we observed along the AP axis. Consistent with this hypothesis are previous studies examining the commitment of neural tissue to particular AP fates. The forebrain becomes committed during early gastrulation (Grinblat et al., 1998), while the hindbrain is committed by mid-gastrulation (Woo and Fraser, 1998), consistent with ventrolateral fates at the MHB position and anteriorly being established by BMP signaling by early gastrulation, whereas hindbrain level ventrolateral fates are not established until mid-gastrulation.

What precludes more posterior ventrolateral cells from being specified by BMP signaling prematurely? This may be the posteriorizing factor alluded to in Nieuwkoop's model. There are a number of candidates for this posteriorizing factor, including Wnt, FGF, and RA. Wnt8 is required for posteriorization of the neurectoderm (Erter et al., 2001; Lekven et al., 2001) and *wnt3a/wnt8* morphants exhibit a dramatic loss of the posterior body (Shimizu et al., 2005). Overexpression of a dominant negative FGF receptor leads to truncation of the body at the level of the first somite (Amaya et al., 1991, Griffin et al., 1995), and inhibits expression of posterior neural markers (Cox and Hemmati-Brivanlou, 1995; Holowacz and Sokol, 1999; Ribisi et al., 2000). RA plays an important role in posteriorizing the hindbrain by directing the expression patterns of a number of transcription factors (reviewed by Moens and Prince, 2002). Components of each of these pathways are expressed in the margin of the embryo at the onset of gastrulation, establishing that they are present at the correct time, and possibly place, to be involved in regulating the competence of a cell to be specified by BMP signaling over time. Overall, our results indicate that two of the embryonic axes are patterned in concert, highlighting the very dynamic, integrative process of axial patterning.

Experimental Procedures

Transgenes

alk8 or *chordin* cDNAs were cloned downstream of the *hsp70/4* promoter (Halloran et al., 2000) creating *hsp70:alk8* and *hsp70:chd*. To generate *Tg(hsp70:alk8)*, 40pg of supercoiled *hsp70*:*alk8* DNA was injected into one-cell stage embryos from a cross of laf^{tm110b}/+ adults and raised to adulthood. F0 founders were intercrossed, and DNA isolated from pools of progeny as described (Connors et al., 2006). Transgene presence was determined by PCR using primers: forward (*hsp70* promoter) TCCCCGACGAGGTGTTTATTC; reverse (*alk8* 225b) GAACAGGATGATGATTTGGG. F0 germ line carriers were crossed to laf^{tm110b}/+ adults and subsequently genotyped for laf^{tm110b}/+ (Mintzer et al., 2001). Both laf^{tm110b} and laf^{m100} are expected null alleles (Bauer et al., 2001, Mintzer et al., 2001). We detected intense, ubiquitous *alk8* expression after a 30 min HS of *Tg(hsp70:alk8)*.

To generate *Tg(hsp70:chd)* lines, 50pg of supercoiled *hsp70*:*chd* DNA was injected into one-cell stage TU WT embryos, which were raised to adulthood, then crossed to each other or to

TU WT fish, progeny heat-shocked at 37° C in a PCR machine, and scored at 24 hpf for dorsalization to identify F0 founders. Of 16 F0 fish screened, two were positive for the transgene, Tg*(hsp70:chd)* line 1 and line 2, and crossed to TU fish to establish an F1 generation. F1 adults were genotyped for the *hsp70:chd* transgene using primers: forward (*hsp70* promoter) TCCCCGACGA GGTGTTTATTC; reverse (*chordin*) CTTGAGTCTCGATCCGTGC.

Heat-shock conditions

For all HS experiments prior to 6 hpf, $snh^{sb1aub}/snh^{sb1aub}$ females (Schmid et al., 2000) were crossed to Tg*(hsp70:chd)* males. For heat-shock experiments after 6 hpf, TU females were crossed to *Tg(hsp70:chd)* males. Embryos were heat-shocked in 100 μl of E3 medium in 96-well plates in a PCR machine. All HS was performed at 37°C for 30 min for Tg*(hsp70:alk8)* and for 1 hour for Tg*(hsp70:chd)*. Following HS, embryos were transferred to Petri dishes with fresh E3 media and kept at 28.5°C.

mRNA injection

Synthetic *alk8* mRNA (100 pg) was injected into one-cell stage embryos from a cross of $laf^{m100}/+$ to$laf^{tm110b}/+$ (Mullins et al., 1996; Solnica-Krezel et al., 1996). Transheterozygous adults were identified by PCR using laf^{tm110b} primers (Mintzer et al., 2001), and the following primers for laf^{m100}: forward (AGAAGACTGTTCATTACCGCGTG); reverse (CCTGTTCAGTGTCAAACTCGTGC), followed by digestion with SalI. Synthetic *bmp2b* mRNA (150 pg) was injected into one-cell stage embryos from crosses of $laf^{tm110b}/$ laf^{m100} females to $laf^{tm110b}/+$ males carrying Tg(*hsp70-alk8*).

Western Blotting

Embryos were prepared as described (Mintzer et al., 2001) with the following changes. After boiling and centrifugation in Laemmli buffer, 1 volume of 1X buffer was added. Samples were subjected to SDS-PAGE analysis on a 10% gel (2 embryos per lane). After transfer to PVDF, membranes were blocked with 5% milk in TBST and probed over two nights with a 1:1000 dilution of anti-phosphoSmad1/5/8 antibody (Cell Signaling Technology) or anti-actin (Sigma) followed by a 1:2000 dilution of goat anti-rabbit antibody and developed using the ECL-Plus kit (Amersham Biosciences) according to manufacturer's instructions. For simplicity, we refer only to P-Smad5 here, although it also includes P-Smad1 in gastrula stages, when it becomes first expressed.

In situ hybridization

Whole-mount in situ hybridizations were performed as described using: *alk8* (Yelick et al., 1998), *chordin* (Miller-Bertoglio et al., 1997), *otx2* (Li et al., 1994), *foxb1.2* (formerly *fkd3*) and *foxd3* (Odenthal and Nusslein-Volhard, 1998), *AP2* (Furthauer et al., 1997), *dlx3* (Akimenko et al., 1994), *gsc* (Stachel et al., 1993), *krox20* (Oxtoby and Jowett, 1993), *myoD* (Weinberg et al., 1996), *pax2.1* (Krauss et al., 1992), *crestin* (Rubinstein et al., 2000), *p63* (Lee and Kimelman, 2002), *WT1* (Serluca and Fishman, 2001) , and *gata1* (Detrich et al., 1995). Embryos were cleared in benzylbenzoate:benzylalcohol (2:1), mounted in Canada balsam, photographed using a Coolsnap camera, images processed using Adobe software.

Immunostaining

Embryos were fixed overnight in 4% PFA at 4° C, blocked in NCS-PBST (10% fetal bovine serum, 1% DMSO, 0.1% Tween-20 in PBS) and probed overnight with a 1:100 dilution of anti-phosphoSmad1/5/8 antibody (Cell Signaling Technology), followed by a 1:500 dilution of goat anti-rabbit Alexa Fluor 488 conjugated antibody (Molecular Probes). Embryos were mounted in Vectashield (Vector Labs), scanned using a Zeiss LSM 510 confocal microscope,

images processed using LSM 510 and Adobe software. Nuclei were visualized with DAPI (Vector Labs) or a 1:10,000 dilution of TO-PRO-3 (Molecular Probes).

Supplementary Material

Refer to Web version on PubMed Central for supplementary material.

Acknowledgements

We thank W. Vought and C. Li for genotyping assistance, J. Villiers for assistance with MZ-*laf* tail rescues, S. Little, T. Gupta and F. Marlow for helpful discussions and critical comments on the manuscript, D. Cobb, J. Hopkins, and E. Fuller for fish facility care. This work was supported by an NIH grant to M.C.M. (GM56326) and NIH training grants (T32 HD0075165 and T32 GM07229-28) to J.A.T., and a fellowship from the American Cancer Society (PF-98-037-01) and NIH training program grant HD07516 to K.A.M.

References

Agathon A, Thisse C, Thisse B. The molecular nature of the zebrafish tail organizer. Nature 2003;424:448–452. [PubMed: 12879074]

Akimenko MA, Ekker M, Wegner J, Lin W, Westerfield M. Combinatorial expression of three zebrafish genes related to distal-less: part of a homeobox gene code for the head. J Neurosci 1994;14:3475–3486. [PubMed: 7911517]

Amaya E, Musci TJ, Kirschner MW. Expression of a dominant negative mutant of the FGF receptor disrupts mesoderm formation in Xenopus embryos. Cell 1991;66:257–270. [PubMed: 1649700]

Bakkers J, Hild M, Kramer C, Furutani-Seiki M, Hammerschmidt M. Zebrafish DeltaNp63 is a direct target of Bmp signaling and encodes a transcriptional repressor blocking neural specification in the ventral ectoderm. Dev Cell 2002;2:617–627. [PubMed: 12015969]

Barth KA, Kishimoto Y, Rohr KB, Seydler C, Schulte-Merker S, Wilson SW. Bmp activity establishes a gradient of positional information throughout the entire neural plate. Development 1999;126:4977–4987. [PubMed: 10529416]

Bauer H, Lele Z, Rauch GJ, Geisler R, Hammerschmidt M. The type I serine/threonine kinase receptor Alk8/Lost-a-fin is required for Bmp2b/7 signal transduction during dorsoventral patterning of the zebrafish embryo. Development 2001;128:849–858. [PubMed: 11222140]

Bonstein L, Elias S, Frank D. Paraxial-fated mesoderm is required for neural crest induction in Xenopus embryos. Dev Biol 1998;193:156–168. [PubMed: 9473321]

Connors SA, Tucker JA, Mullins MC. Temporal and spatial action of Tolloid (Mini fin) and Chordin to pattern tail tissues. Dev Biol 2006;293:191–202. [PubMed: 16530746]

Cox WG, Hemmati-Brivanlou A. Caudalization of neural fate by tissue recombination and bFGF. Development 1995;121:4349–4358. [PubMed: 8575335]

Detrich HW 3rd, Kieran MW, Chan FY, Barone LM, Yee K, Rundstadler JA, Pratt S, Ransom D, Zon LI. Intraembryonic hematopoietic cell migration during vertebrate development. Proc Natl Acad Sci U S A 1995;92:10713–10717. [PubMed: 7479870]

Dick A, Hild M, Bauer H, Imai Y, Maifeld H, Schier AF, Talbot WS, Bouwmeester T, Hammerschmidt M. Essential role of Bmp7 (snailhouse) and its prodomain in dorsoventral patterning of the zebrafish embryo. Development 2000;127:343–354. [PubMed: 10603351]

Dosch R, Gawantka V, Delius H, Blumenstock C, Niehrs C. Bmp-4 acts as a morphogen in dorsoventral mesoderm patterning in Xenopus. Development 1997;124:2325–2334. [PubMed: 9199359]

Erter CE, Wilm TP, Basler N, Wright CV, Solnica-Krezel L. Wnt8 is required in lateral mesendodermal precursors for neural posteriorization in vivo. Development 2001;128:3571–3583. [PubMed: 11566861]

Faure S, Lee MA, Keller T, ten Dijke P, Whitman M. Endogenous patterns of TGFbeta superfamily signaling during early Xenopus development. Development 2000;127:2917–2931. [PubMed: 10851136]

Furthauer M, Thisse C, Thisse B. A role for FGF-8 in the dorsoventral patterning of the zebrafish gastrula. Development 1997;124:4253–4264. [PubMed: 9334274]

Gamse J, Sive H. Vertebrate anteroposterior patterning: the Xenopus neurectoderm as a paradigm. Bioessays 2000;22:976–986. [PubMed: 11056474]

Gamse JT, Sive H. Early anteroposterior division of the presumptive neurectoderm in Xenopus. Mech Dev 2001;104:21–36. [PubMed: 11404077]

Griffin K, Patient R, Holder N. Analysis of FGF function in normal and no tail zebrafish embryos reveals separate mechanisms for formation of the trunk and the tail. Development 1995;121:2983–2994. [PubMed: 7555724]

Grinblat Y, Gamse J, Patel M, Sive H. Determination of the zebrafish forebrain: induction and patterning. Development 1998;125:4403–4416. [PubMed: 9778500]

Gritsman K, Zhang J, Cheng S, Heckscher E, Talbot WS, Schier AF. The EGF-CFC protein one-eyed pinhead is essential for nodal signaling. Cell 1999;97:121–132. [PubMed: 10199408]

Halloran MC, Sato-Maeda M, Warren JT, Su F, Lele Z, Krone PH, Kuwada JY, Shoji W. Laser-induced gene expression in specific cells of transgenic zebrafish. Development 2000;127:1953–1960. [PubMed: 10751183]

Harfe BD, Scherz PJ, Nissim S, Tian H, McMahon AP, Tabin CJ. Evidence for an expansion-based temporal Shh gradient in specifying vertebrate digit identities. Cell 2004;118:517–528. [PubMed: 15315763]

Holowacz T, Sokol S. FGF is required for posterior neural patterning but not for neural induction. Dev Biol 1999;205:296–308. [PubMed: 9917365]

Kimmel CB, Warga RM, Schilling TF. Origin and organization of the zebrafish fate map. Development 1990;108:581–594. [PubMed: 2387237]

Kishimoto Y, Lee KH, Zon L, Hammerschmidt M, Schulte-Merker S. The molecular nature of zebrafish swirl: BMP2 function is essential during early dorsoventral patterning. Development 1997;124:4457–4466. [PubMed: 9409664]

Knecht AK, Harland RM. Mechanisms of dorsal-ventral patterning in noggin-induced neural tissue. Development 1997;124:2477–2488. [PubMed: 9199373]

Kozlowski DJ, Murakami T, Ho RK, Weinberg ES. Regional cell movement and tissue patterning in the zebrafish embryo revealed by fate mapping with caged fluorescein. Biochem Cell Biol 1997;75:551–562. [PubMed: 9551179]

Krauss S, Maden M, Holder N, Wilson SW. Zebrafish pax[b] is involved in the formation of the midbrain-hindbrain boundary. Nature 1992;360:87–89. [PubMed: 1436081]

Kudoh T, Wilson SW, Dawid IB. Distinct roles for Fgf, Wnt and retinoic acid in posteriorizing the neural ectoderm. Development 2002;129:4335–4346. [PubMed: 12183385]

LaBonne C, Bronner-Fraser M. Neural crest induction in Xenopus: evidence for a two-signal model. Development 1998;125:2403–2414. [PubMed: 9609823]

Lee H, Kimelman D. A dominant-negative form of p63 is required for epidermal proliferation in zebrafish. Dev Cell 2002;2:607–616. [PubMed: 12015968]

Lekven AC, Thorpe CJ, Waxman JS, Moon RT. Zebrafish wnt8 encodes two wnt8 proteins on a bicistronic transcript and is required for mesoderm and neurectoderm patterning. Dev Cell 2001;1:103–114. [PubMed: 11703928]

Lane MC, Sheets MD. Heading in a new direction: Implications of the revised fate map for understanding *Xenopus laevis* development. Dev Biol 2006;296:12–28. [PubMed: 16750823]

Li Y, Allende ML, Finkelstein R, Weinberg ES. Expression of two zebrafish orthodenticle-related genes in the embryonic brain. Mech Dev 1994;48:229–244. [PubMed: 7893604]

Little SC, Mullins MC. Extracellular modulation of BMP activity in patterning the dorsoventral axis. Birth Defects Res C Embryo Today 2006;78:224–242. [PubMed: 17061292]

Marchant L, Linker C, Ruiz P, Guerrero N, Mayor R. The inductive properties of mesoderm suggest that the neural crest cells are specified by a BMP gradient. Dev Biol 1998;198:319–329. [PubMed: 9659936]

Marom K, Levy V, Pillemer G, Fainsod A. Temporal analysis of the early BMP functions identifies distinct anti-organizer and mesoderm patterning phases. Dev Biol 2005;282:442–454. [PubMed: 15950609]

Maves L, Kimmel CB. Dynamic and sequential patterning of the zebrafish posterior hindbrain by retinoic acid. Dev Biol 2005;285:593–605. [PubMed: 16102743]

Miller-Bertoglio VE, Fisher S, Sanchez A, Mullins MC, Halpern ME. Differential regulation of chordin expression domains in mutant zebrafish. Dev Biol 1997;192:537–550. [PubMed: 9441687]

Mintzer KA, Lee MA, Runke G, Trout J, Whitman M, Mullins MC. Lost-a-fin encodes a type I BMP receptor, Alk8, acting maternally and zygotically in dorsoventral pattern formation. Development 2001;128:859–869. [PubMed: 11222141]

Moens CB, Prince VE. Constructing the hindbrain: insights from the zebrafish. Dev Dyn 2002;224:1–17. [PubMed: 11984869]

Mullins MC, Hammerschmidt M, Kane DA, Odenthal J, Brand M, van Eeden FJ, Furutani-Seiki M, Granato M, Haffter P, Heisenberg CP, et al. Genes establishing dorsoventral pattern formation in the zebrafish embryo: the ventral specifying genes. Development 1996;123:81–93. [PubMed: 9007231]

Myers DC, Sepich DS, Solnica-Krezel L. Bmp activity gradient regulates convergent extension during zebrafish gastrulation. Dev Biol 2002;243:81–98. [PubMed: 11846479]

Neave B, Holder N, Patient R. A graded response to BMP-4 spatially coordinates patterning of the mesoderm and ectoderm in the zebrafish. Mech Dev 1997;62:183–195. [PubMed: 9152010]

Nguyen M, Park S, Marques G, Arora K. Interpretation of a BMP activity gradient in Drosophila embryos depends on synergistic signaling by two type I receptors, SAX and TKV. Cell 1998a;95:495–506. [PubMed: 9827802]

Nguyen VH, Schmid B, Trout J, Connors SA, Ekker M, Mullins MC. Ventral and lateral regions of the zebrafish gastrula, including the neural crest progenitors, are established by a bmp2b/swirl pathway of genes. Dev Biol 1998b;199:93–110. [PubMed: 9676195]

Nguyen VH, Trout J, Connors SA, Andermann P, Weinberg E, Mullins MC. Dorsal and intermediate neuronal cell types of the spinal cord are established by a BMP signaling pathway. Development 2000;127:1209–1220. [PubMed: 10683174]

O'Connor MB, Umulis D, Othmer HG, Blair SS. Shaping BMP morphogen gradients in the Drosophila embryo and pupal wing. Development 2006;133:183–193. [PubMed: 16368928]

Odenthal J, Nusslein-Volhard C. fork head domain genes in zebrafish. Dev Genes Evol 1998;208:245–258. [PubMed: 9683740]

Oxtoby E, Jowett T. Cloning of the zebrafish krox-20 gene (krx-20) and its expression during hindbrain development. Nucleic Acids Res 1993;21:1087–1095. [PubMed: 8464695]

Pyati UJ, Webb AE, Kimelman D. Transgenic zebrafish reveal stage-specific roles for Bmp signaling in ventral and posterior mesoderm development. Development 2005;132:2333–2343. [PubMed: 15829520]

Ragland JW, Raible DW. Signals derived from the underlying mesoderm are dispensable for zebrafish neural crest induction. Dev Biol 2004;276:16–30. [PubMed: 15531361]

Reversade B, De Robertis EM. Regulation of ADMP and BMP2/4/7 at opposite embryonic poles generates a self-regulating morphogenetic field. Cell 2005;123:1147–1160. [PubMed: 16360041]

Reversade B, Kuroda H, Lee H, Mays A, De Robertis EM. Depletion of Bmp2, Bmp4, Bmp7 and Spemann organizer signals induces massive brain formation in Xenopus embryos. Development 2005;132:3381–3392. [PubMed: 15975940]

Ribisi S Jr. Mariani FV, Aamar E, Lamb TM, Frank D, Harland RM. Ras-mediated FGF signaling is required for the formation of posterior but not anterior neural tissue in Xenopus laevis. Dev Biol 2000;227:183–196. [PubMed: 11076686]

Rubinstein AL, Lee D, Luo R, Henion PD, Halpern ME. Genes dependent on zebrafish cyclops function identified by AFLP differential gene expression screen. Genesis 2000;26:86–97. [PubMed: 10660676]

Sander K. Specification of the basic body pattern in insect embryogenesis. Adv. Insect Physiol 1976;12:125–238.

Schmid B, Furthauer M, Connors SA, Trout J, Thisse B, Thisse C, Mullins MC. Equivalent genetic roles for bmp7/snailhouse and bmp2b/swirl in dorsoventral pattern formation. Development 2000;127:957–967. [PubMed: 10662635]

Schohl A, Fagotto F. Beta-catenin, MAPK and Smad signaling during early Xenopus development. Development 2002;129:37–52. [PubMed: 11782399]

Serluca FC, Fishman MC. Pre-pattern in the pronephric kidney field of zebrafish. Development 2001;128:2233–2241. [PubMed: 11493543]

Sepich DS, Myers DC, Short R, Topczewski J, Marlow F, Solnica-Krezel L. Role of the zebrafish trilobite locus in gastrulation movements of convergence and extension. Genesis 2000;4:159–173. [PubMed: 10992326]

Shimizu T, Bae YK, Muraoka O, Hibi M. Interaction of Wnt and caudal-related genes in zebrafish posterior body formation. Dev Biol 2005;279:125–141. [PubMed: 15708563]

Solnica-Krezel L, Stemple DL, Mountcastle-Shah E, Rangini Z, Neuhauss SC, Malicki J, Schier AF, Stainier DY, Zwartkruis F, Abdelilah S, Driever W. Mutations affecting cell fates and cellular rearrangements during gastrulation in zebrafish. Development 1996;123:67–80. [PubMed: 9007230]

Stachel SE, Grunwald DJ, Myers PZ. Lithium perturbation and goosecoid expression identify a dorsal specification pathway in the pregastrula zebrafish. Development 1993;117:1261–1274. [PubMed: 8104775]

Stern CD, Charite J, Deschamps J, Duboule D, Durston AJ, Kmita M, Nicolas JF, Palmeirim I, Smith JC, Wolpert L. Head-tail patterning of the vertebrate embryo: one, two or many unresolved problems? Int J Dev Biol 2006;50:3–15. [PubMed: 16323073]

Tribulo C, Aybar MJ, Nguyen VH, Mullins MC, Mayor R. Regulation of Msx genes by a Bmp gradient is essential for neural crest specification. Development 2003;130:6441–6452. [PubMed: 14627721]

Von der Hardt S, Bakkers J, Inbal A, Carvalho L, Solnica-Krezel L, Heisenberg CP, Hammerschmidt M. The Bmp gradient of the zebrafish gastrula guides migrating lateral cells by regulating cell-cell adhesion. Curr Biol 2007;17:475–487. [PubMed: 17331724]

Wawersik S, Evola C, Whitman M. Conditional BMP inhibition in Xenopus reveals stage-specific roles for BMPs in neural and neural crest induction. Dev Biol 2005;277:425–442. [PubMed: 15617685]

Weinberg ES, Allende ML, Kelly CS, Abdelhamid A, Murakami T, Andermann P, Doerre OG, Grunwald DJ, Riggleman B. Developmental regulation of zebrafish MyoD in wild-type, no tail and spadetail embryos. Development 1996;122:271–280. [PubMed: 8565839]

Wilson PA, Lagna G, Suzuki A, Hemmati-Brivanlou A. Concentration-dependent patterning of the Xenopus ectoderm by BMP4 and its signal transducer Smad1. Development 1997;124:3177–3184. [PubMed: 9272958]

Woo K, Fraser SE. Order and coherence in the fate map of the zebrafish nervous system. Development 1995;121:2595–2609. [PubMed: 7671822]

Woo K, Fraser SE. Specification of the hindbrain fate in the zebrafish. Dev Biol 1998;197:283–296. [PubMed: 9630752]

Yelick PC, Abduljabbar TS, Stashenko P. zALK-8, a novel type I serine/threonine kinase receptor, is expressed throughout early zebrafish development. Dev Dyn 1998;211:352–361. [PubMed: 9566954]

Zhao G. Consequences of knocking out BMP signaling in the mouse. Genesis 2003;35:43–56. [PubMed: 12481298]

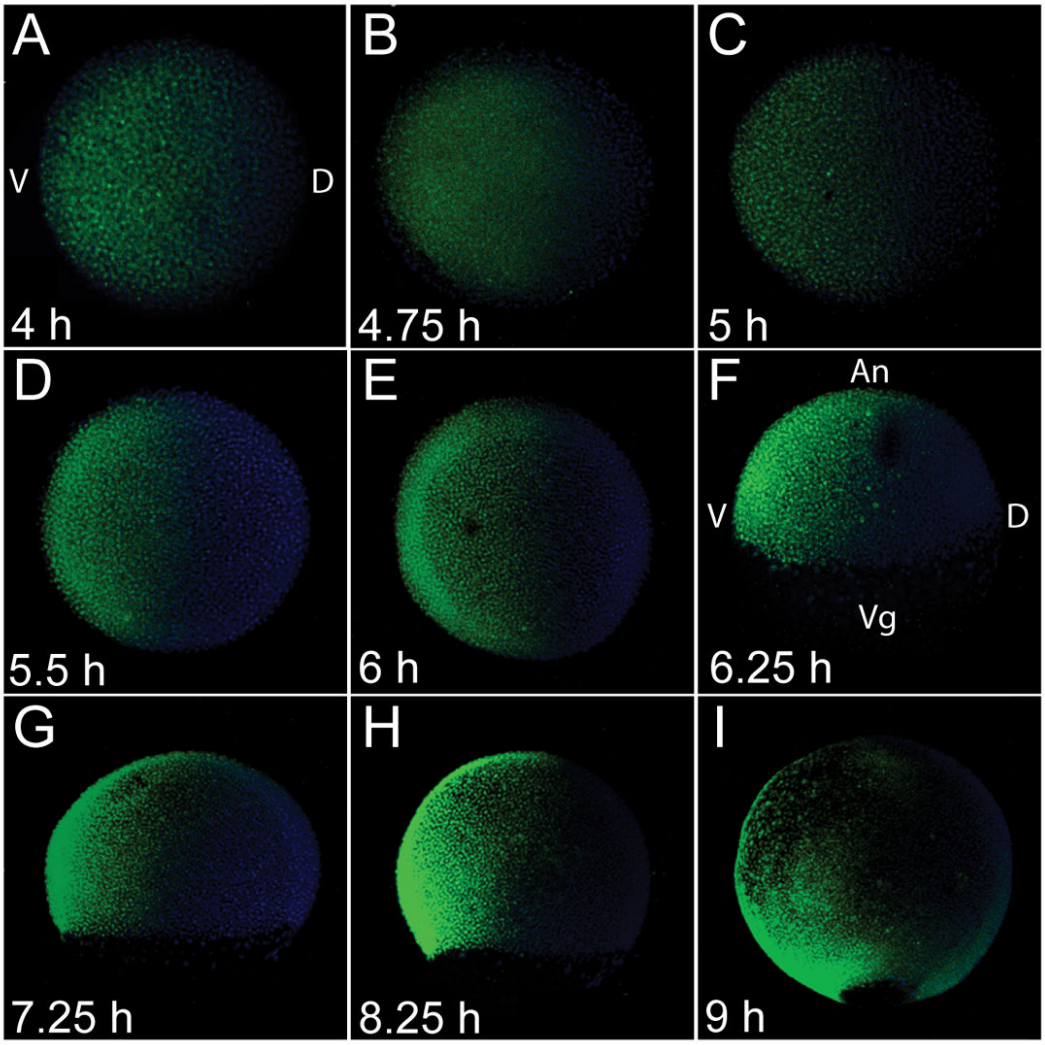

Fig 1.

Formation of the BMP activity gradient. Wholemount P-Smad5 (green) antibody staining during blastula stages, at 4 hpf (A), 4.75 hpf (B), 5 hpf (C) and during gastrula stages at 5.5 hpf (D), 6 hpf (E), 6.25 hpf (F), 7.25 hpf (G), 8.25 hpf (H), and 9 hpf (I). Nuclei were stained with DAPI (blue). A-E animal view, F-I, lateral view, dorsal to right in all.

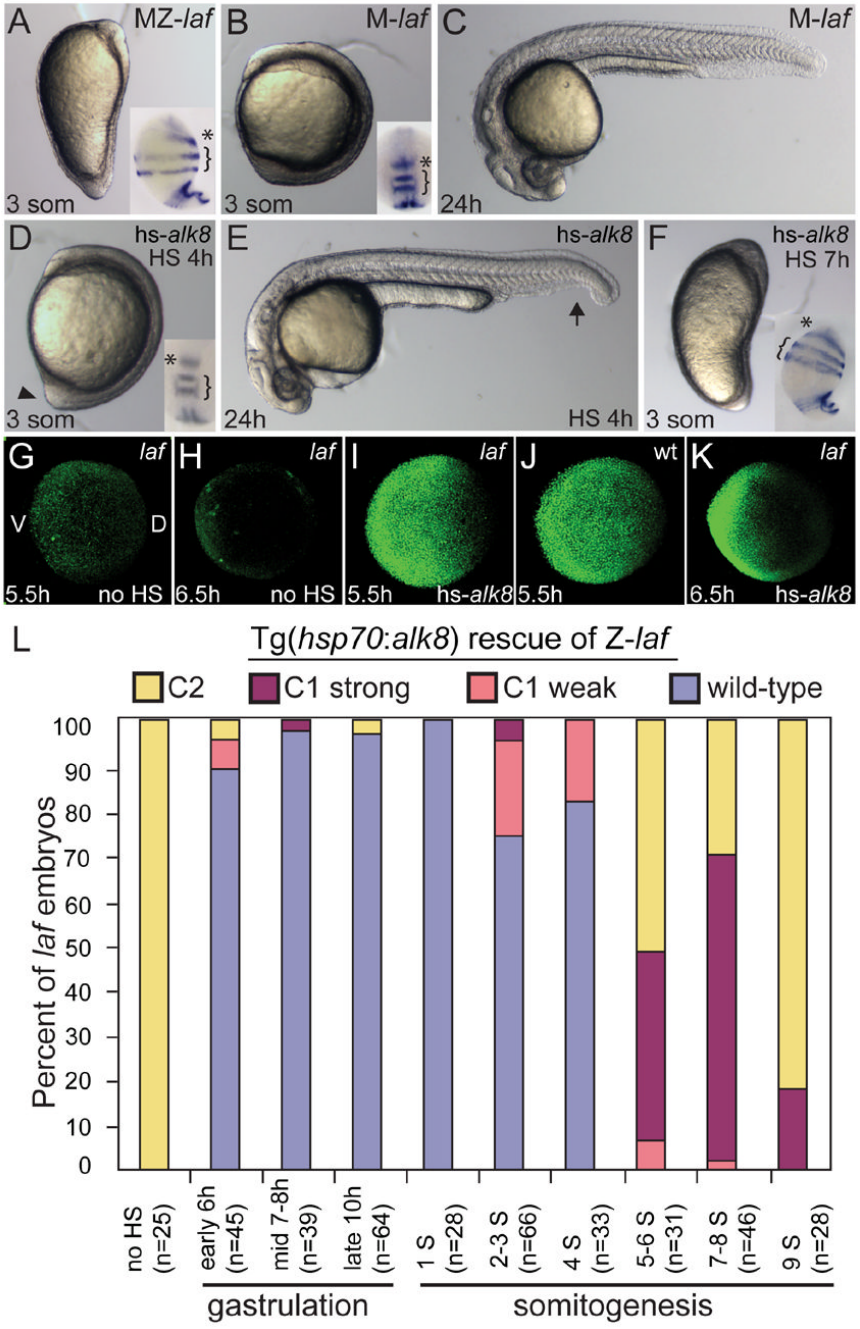

Fig 2.

Temporal series of Tg(*hsp70*:*alk8*) induction to rescue MZ-*laf* and Z-*laf*. Live C5 dorsalized non-heat-shocked MZ-*laf* transgenic embryo at the 3-somite (3 som) stage (A). Live M-*laf* embryos (*laf*/+ embryos from *laf*/*laf* mother) heat-shocked at 4 hpf display a wild-type (WT) phenotype at the 3-som stage (B) and at 24 hpf (C), consistent with a lack of *alk8* overexpression phenotypic effects (Bauer et al., 2001; Mintzer et al., 2001). HS (Heat-shock) of MZ-*laf;* Tg (*hsp70*:*alk8*)/+ embryos at 4 hpf rescues them to C1 phenotype (D, arrowhead marks protruding tail bud; E, arrow marks partial loss of the ventral tail fin). HS at 7 hpf (F) fails to rescue MZ-*laf* transgenic embryos. MZ-*laf* mutants vary in the expansion of *pax2.1* expression in the MHB (*), from greatly expanded (A inset) to circumferential (F inset). P-Smad5 in non-heat-shocked

MZ-*laf* embryos at 5.5 hpf (G) and 6.5 hpf (H). After HS at 5 hpf, P-Smad5 at 5.5 hpf (I) and 6.5 hpf (K) in MZ-*laf* and WT (J). A higher gain was used to image all P-Smad5 embryos in this figure compared to Fig 1. (L) Graphic of extent of rescue of zygotic *laf* mutant transgenic embryos heat-shocked for 30 min at different time points. G, H-K are animal views, dorsal to right, insets in B, D are dorsal views, anterior to top, all others are lateral views, dorsal to right. Insets in A, B, D, F are *pax2.1* (asterisk), *krox20* (bracket) and *myoD* in situ hybridization at the 5-somite stage.

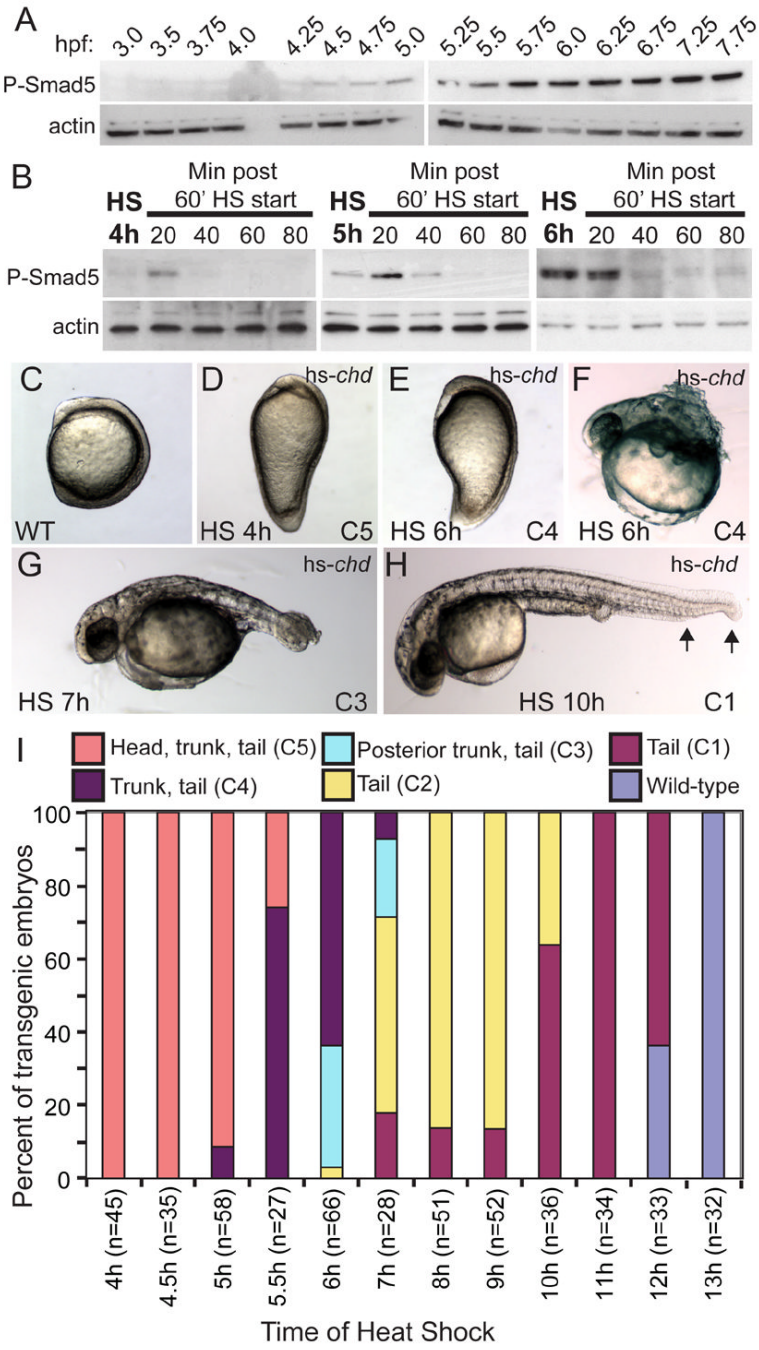

Fig 3.

Tg(*hsp70*:*chd*) rapidly inhibits BMP signaling, generating a range of dorsalized phenotypes dependent on induction time. (A) P-Smad5 Western blot at blastula (3.0 to 5.25 hpf), onset of gastrulation (5.5 hpf) through mid-gastrulation (5.75 to 7.75 hpf) stages. (B) P-Smad5 during (20, 40 min time points) and immediately after a 60-min HS at 4, 5, or 6 hpf. Actin is a loading control. Non-transgenic WT (C), and transgenic siblings heat-shocked at 4 hpf (D) or 6 hpf (E) at the 3-somite stage and at 1 dpf (F). Dorsalization at 1 dpf of embryos heat-shocked at 7 hpf (G) and 10 hpf (H, arrows indicate loss of ventral tail tissue). (I) Distribution of dorsalized phenotypes following HS at different time points.

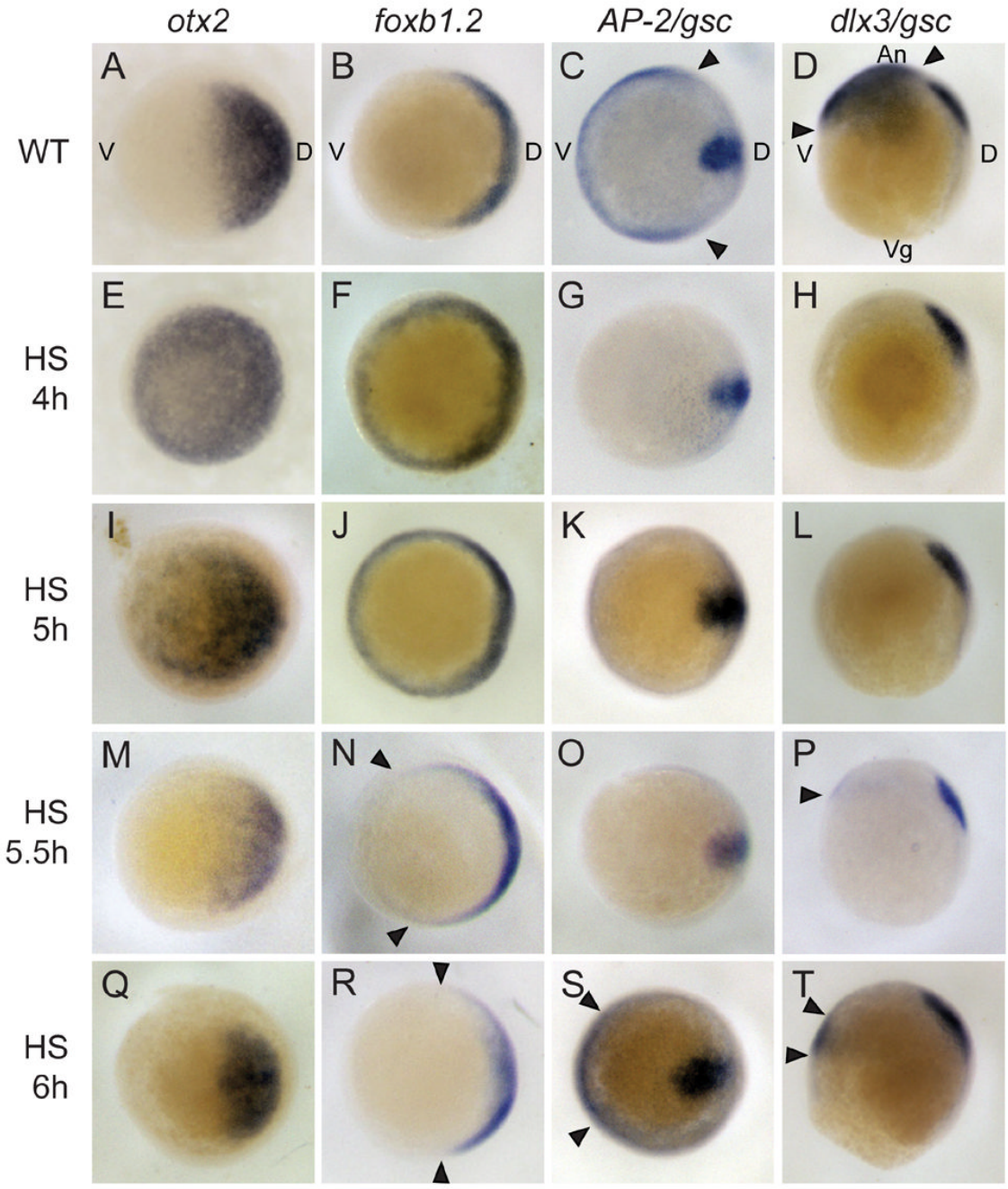

Fig 4.

Tg(*hsp70:chd*) induced dorsalization is apparent during gastrulation. Whole mount in situ hybridization of non-transgenic heat-shocked WT siblings (A-D) compared to heat-shocked transgenic embryos (E-T). *otx2* expression at 60-65% epiboly in prospective anterior neural tissue in WT (A), or transgenic following HS at 4 hpf (E, n=9/9), 5 hpf (I, n=6/6), 5.5 hpf (M, n=19/19) or 6 hpf (Q, n=13/13). *foxb1.2* expression in prospective neurectoderm in WT at 50% epiboly (B), or at 50% epiboly or shield stage immediately following HS at 4 hpf (F, n=3/3) or 5 hpf (J, n=9/9), respectively. *foxb1.2* expression at 55-60% epiboly following a 5.5 hpf HS (N, n=9/10), and at 65-70% epiboly following a 6 hpf HS (R, n=15/15). *AP2* expression at 70% epiboly in ventral non-neural ectoderm in WT (C), and following HS at 4 hpf (G, n=13/13), 5

hpf (K, n=7/7), 5.5 hpf (O, n=7/7), or 6 hpf (S, n=8/8). *dlx3* expression at 70% epiboly in ventral non-neural ectoderm in WT (D), and following HS at 4 hpf (H, n=12/12), 5 hpf (L, n=7/7), 5.5 hpf (P, n=8/10) or 6 hpf (T, n=12/16). *gsc* expression in dorsal midline mesoderm serves as a control for *AP-2* and *dlx-3*, and is unaffected by HS. Arrowheads denote expression domains. D, H, L, P, T lateral views, dorsal to right, all others are animal views, dorsal to right.

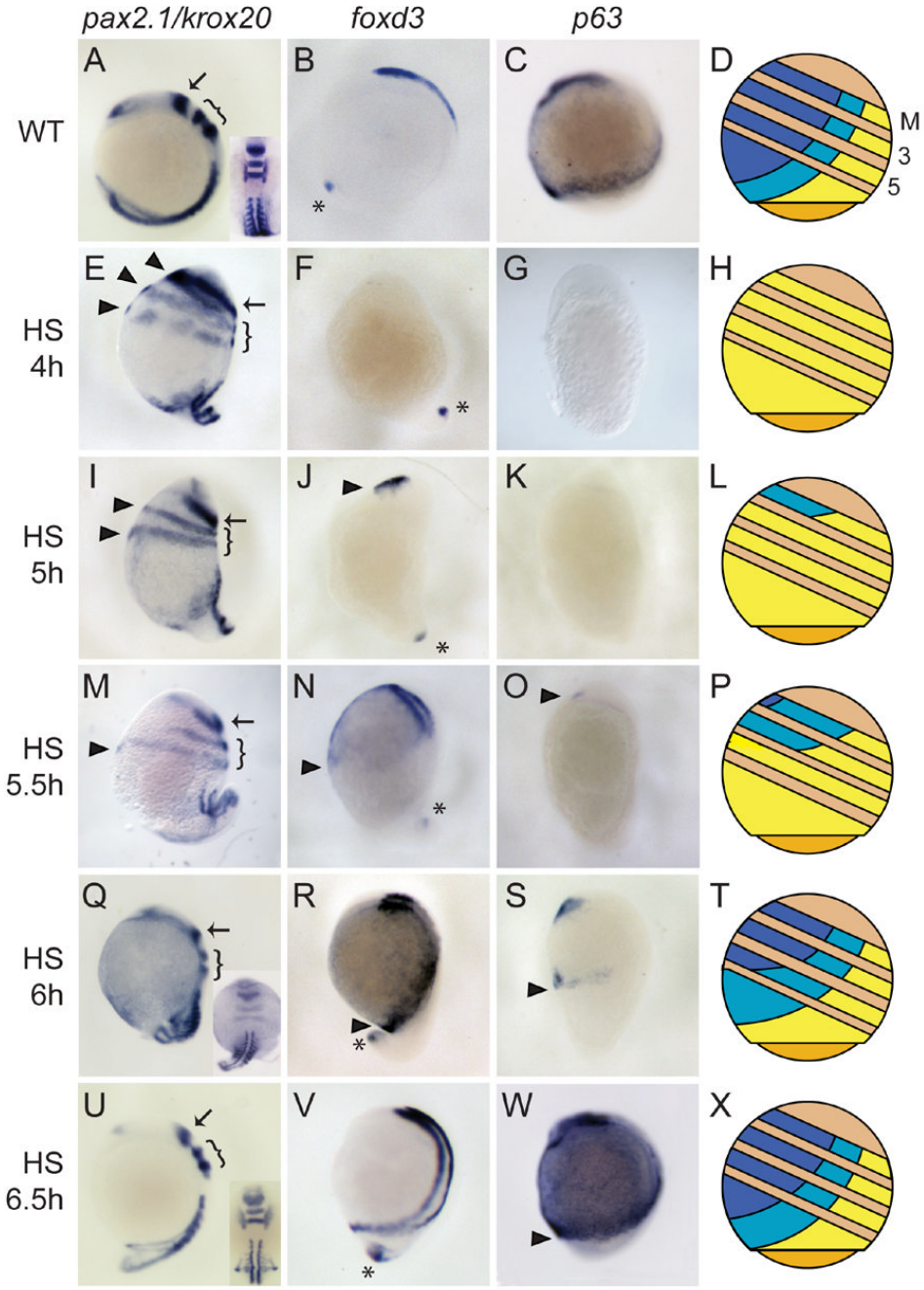

Fig 5.

Progressive BMP inhibition series by Tg(*hsp70:chd*) reveals progressive DV ectodermal patterning along the AP axis. Expression of *pax2.1* in the MHB (arrow), *krox20* in R3 and R5 (bracket), and *myoD* in somitic mesoderm at the 6-somite stage in WT (A) and following HS at 4 hpf (E, n=17/19), 5 hpf (I, n=15/21), 5.5 hpf (M, n=13/18), 6 hpf (Q, n=21/21), or 6.5 hpf (U, n=11/11). Arrowheads denote circumferential neural tissues. *foxd3* expression in CNC at the 6-somite stage in WT (B) and following HS at 4 hpf (F, n=12/13), 5 hpf (J, n=13/21), 5.5 hpf (N, n=15/19), 6 hpf (R, n=11/15), or 6.5 hpf (V). Asterisks denote unaffected tail bud expression. *p63* expression in prospective epidermis at the 2-somite stage in WT (C) and following HS at 4 hpf (G, n=8/8), 5 hpf (K, n=16/16), 5.5 hpf (O, n=8/17), 6 hpf (S, n=16/24),

or 6.5 hpf (W, n=5/5). (D, H, L, P, T, X) Representations summarize the relative domains of the three tissue types. Yellow is neurectoderm, turquoise is neural crest, and blue is epidermis. M indicates MHB boundary, 3 and 5 are R3 and R5. Tan stripes are the regions between the MHB, R3, and R5 AP positions across the DV axis. All are lateral views, dorsal to right, anterior to top, except insets in A, Q, U, which are dorsal views, anterior to top.

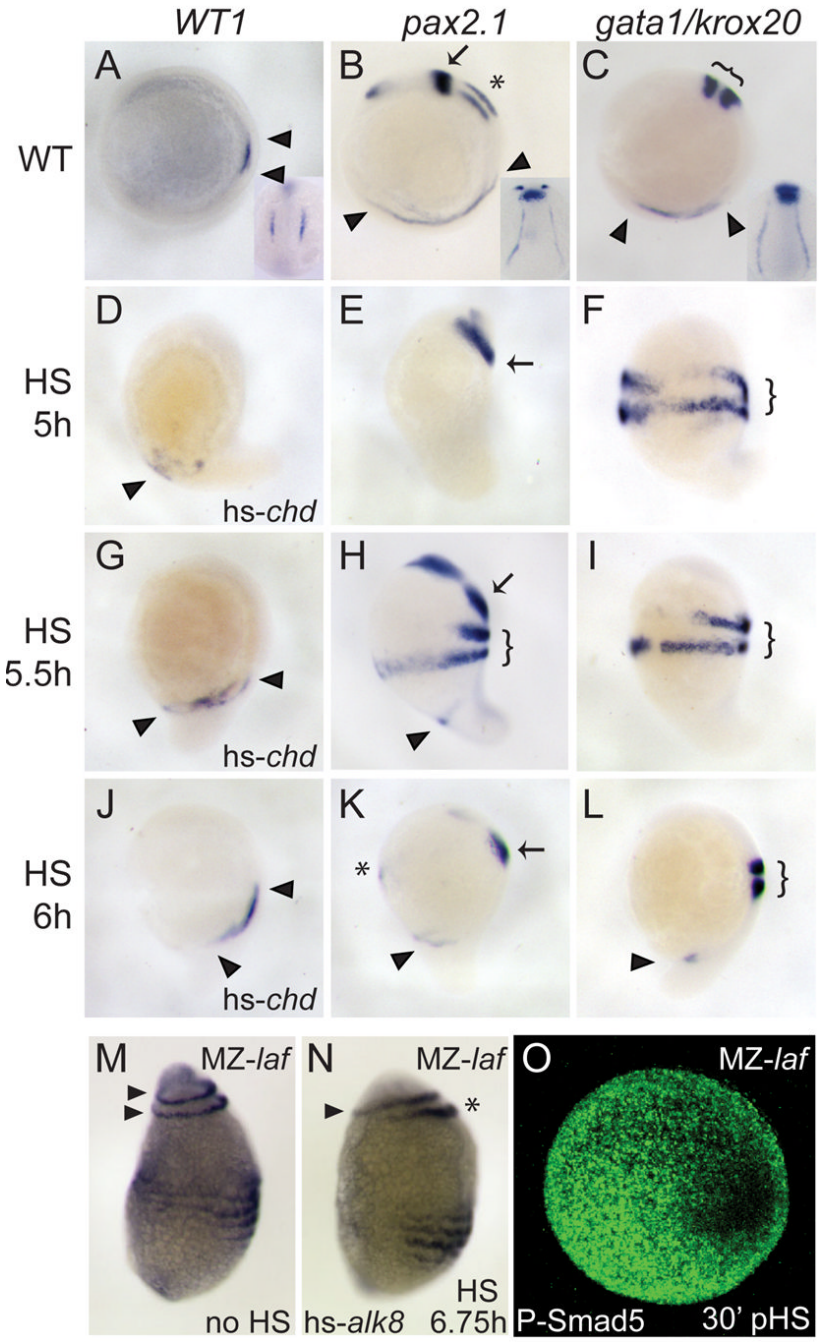

Fig 6.

Progressive BMP inhibition series reveals progressive DV mesodermal patterning along the AP axis, and rescue of posterior but not anterior in MZ-*laf* embryos. *WT1* expression in the pronephros in heat-shocked non-transgenic WT siblings (A), and following HS at 5 hpf (D, n=16/19), 5.5 hpf (G, n=7/12), or 6 hpf (J, n=10/12). *pax2.1* expression in pronephros (arrowheads), MHB (arrow), and otic placode (asterisk) in WT (B), and following HS at 5 hpf (E, n=16/16), 5.5 hpf (H, n=14/24), or 6 hpf (K, n=10/13). *krox20* expression was also examined in H (brackets). Expression of *gata1* in blood progenitors (arrowheads) and *krox20* in hindbrain (brackets) in WT (C) and following HS at 5 hpf (F, n=5/5), 5.5 hpf (I, n=6/6), or 6 hpf (L, n=5/7). (M) *krox20* expression in R3 and R5 (arrowheads), and *myoD* in somitic mesoderm in

MZ-*laf* mutants overexpressing *bmp2b* in the absence of HS (M) or following a 30-min HS induction at 6.75 hpf (N) of Tg(*hsp70*:*alk8*) causes partial expansion of R5 (asterisk), but complete expansion of R3 (arrowhead), and re-initiation of P-Smad5 by 7.25 hpf (O). A-N are lateral views, dorsal to right, at 5-somite stage. O is animal pole view, dorsal to right.

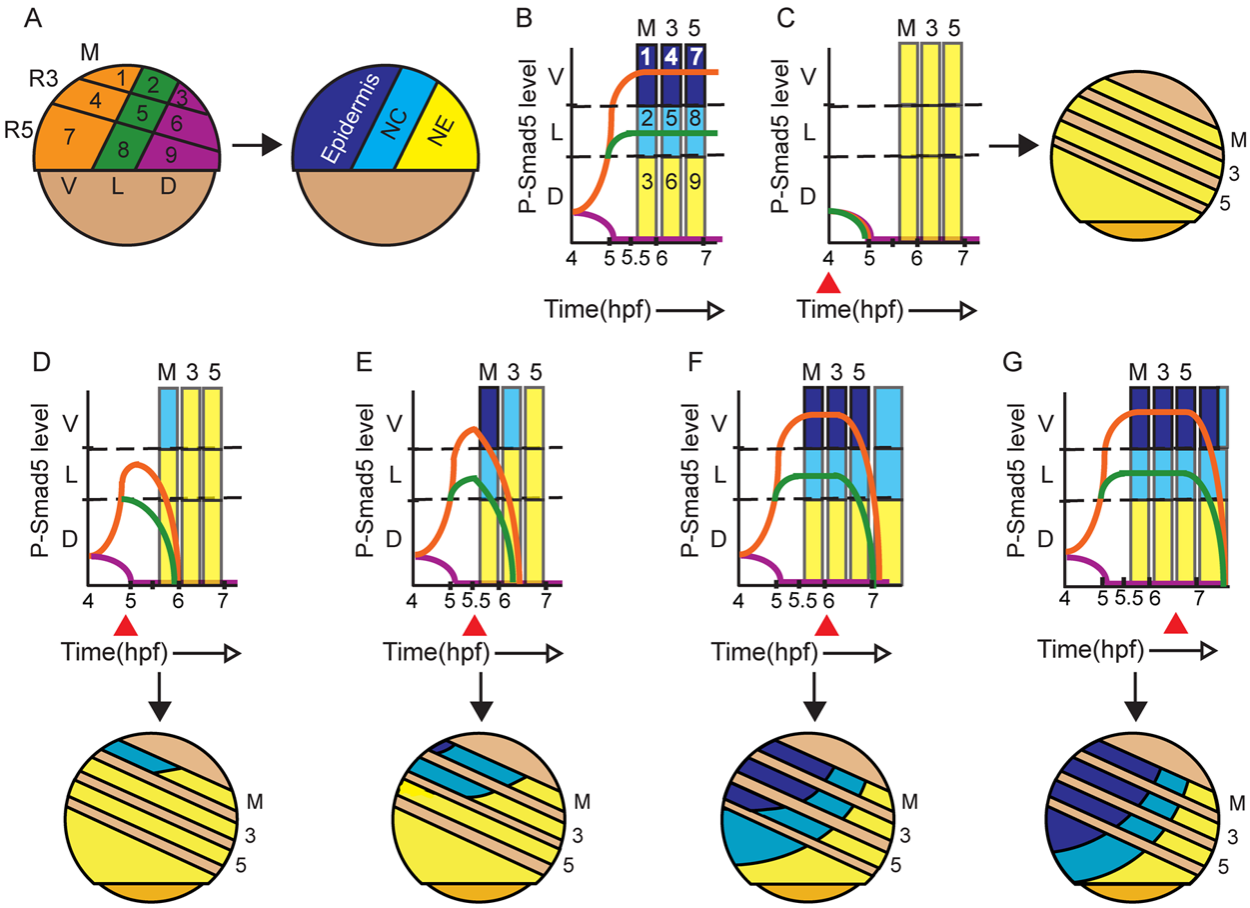

Fig 7.

Progressive Critical Intervals Model.

(A) In the left embryo schematic orange (1, 4, 7), green (2, 5, 8), and purple (3, 6, 9) represent ventral, lateral, and dorsal positions in the embryo, respectively. M (MHB, 1, 2, 3), R3 (4, 5, 6) and R5 (7, 8, 9) represent different AP positions. Right embryo schematic shows the DV cell fate that normally forms from each DV position. (B) P-Smad5 levels are shown over time for three discrete ventral (V), lateral (L), and dorsal (D) positions (colored lines), giving rise to three different cell fates. Color scheme as in (A). The critical interval for BMP signal interpretation for each AP position is indicated by the vertical rectangle. (C-G) Plots of P-Smad5 levels following each HS induction time point, as indicated by the red triangle, for each DV position over time. Changes in DV cell fate for each AP position are indicated by the box color in the rectangles and in the schematized embryos below.